Interleaved and partial transmission interleaved optical coherent orthogonal frequency division multiplexing

Interleaved and partial transmission interleaved optical coherent orthogonal frequency division multiplexing

Zizheng Cao,* Henrie P. A. van den Boom, Eduward Tangdiongga, and Ton Koonen

COBRA Institute, Eindhoven University of Technology, NL 5600 MB Eindhoven, The Netherlands

**Corresponding author: z.cao@tue.nl*

Received December 27, 2013; revised February 26, 2014; accepted March 7, 2014; posted March 7, 2014 (Doc. ID 203748); published March 31, 2014

A novel group of interleaved orthogonal frequency division multiplexing (IL-OFDM) and partial transmission IL-OFDM (PT-IL-OFDM) schemes are proposed for optical coherent detection. In the interleaved operation, the odd (or even) subcarriers of an OFDM symbol are reserved (closed). Such an interleaved arrangement can gain the tolerance toward phase noise induced interchannel interference (PN-ICI). Meanwhile, the peak to average power ratio (PAPR) of an OFDM signal can be significantly reduced. However, half of the capacity is sacrificed for the interleaved operation. By exploring the time domain symmetry property of IL-OFDM, the concept of PT-IL-OFDM is proposed to double the capacity of IL-OFDM. Consequently, PT-IL-OFDM can gain the merits of low PAPR and a high tolerance toward PN-ICI without capacity sacrifice. Numerical simulation verified the advanced properties of IL-OFDM and PT-IL-OFDM.

OCIS codes: (060.2330) Fiber optics communications; (060.1660) Coherent communications; (060.2920) Homodyning.
http://dx.doi.org/10.1364/OL.39.002179

Optical coherent orthogonal frequency division multiplexing (OFDM) has been proposed and intensely investigated for optical transmission systems [1–11] and optical access networks [12–16] due to its high spectral efficiency, robustness toward fiber chromatic dispersion and polarization mode dispersion, and capability of dynamic bandwidth allocation. However, optical coherent OFDM is vulnerable for the interchannel interference (ICI) induced by PN and frequency offsets between the arriving optical signal and the optical local oscillator (OLO). Apart from frequency offsets, which can be efficiently compensated for, the phase noise induced ICI (rather than common phase error, CPE) is difficult to deal with. Moreover, the high peak to average power ratio (PAPR) increases the nonlinear distortion at both transceivers and optical fiber links. Many schemes are proposed to reduce the phase noise induced ICI (PN-ICI) in optical coherent OFDM systems. Among them, the RF pilot scheme is widely considered as the most practical method [7]. However, in such a scheme, a DC bias offset from the optical carrier suppression point is required, which results in the asymmetric distortion of the OFDM signal. For the PAPR reduction, the digital Fourier transform (DFT) spreading scheme has attracted a lot of attention due to its capability to largely reduce the PAPR [11]. However, the two additional operations of DFT and IDFT (inverse digital Fourier transform) significantly increase the complexity. In this Letter, the interleaved OFDM (IL-OFDM) is proposed to reduce the PAPR and to enhance the tolerance toward PN-ICI with half-subcarriers reserved. Then, the concept of partial transmission IL-OFDM (PT-IL-OFDM) is proposed to double the capacity of IL-OFDM by exploring its symmetry property. Moreover, the proposed concepts introduce negligible additional complexity and are also compatible with the aforementioned schemes to reduce PN-ICI and PAPR.

The phase noise induced ICIs for T-OFDM (traditional OFDM) are shown in Fig. 1, labeled as "T-OFDM". The arrows represent the subcarriers of the OFDM signal in the frequency domain. In the frequency domain, the phase noise is modulated to each subcarrier and spreads to other subcarriers, which causes the ICI. The spectral profile of the laser phase noise is schematically labeled in Fig. 1. It can be written as

$$S_\rho(f) = \frac{\alpha}{2\pi f^2}, \tag{1}$$

where α denotes the combined FWHM linewidth of the transmit and receive lasers. Its low-pass feature shows that most energy of the phase noise, ρ_Δ, exists near its central frequency. In other words, the main ICI contributions to one subcarrier are from its neighboring subcarriers. As shown in Fig. 1, the bell-shape dashed lines represent the ICI from one subcarrier to all other subcarriers. For a given subcarrier we can clearly see that the most ICI contributions are from its neighboring subcarriers. For the IL-OFDM (labeled as "IL-OFDM" in Fig. 1), only the odd or even subcarriers carry data and the others are closed. Thus, the PN-ICI is much reduced.

Now, we discuss the realization of a PT-IL-OFDM signal based on IDFT/DFT. First, we discuss the generation of an IL-OFDM signal, and then we explore its symmetry property to produce a PT-IL-OFDM signal. The IDFT realization of an IL-OFDM signal can be expressed as:

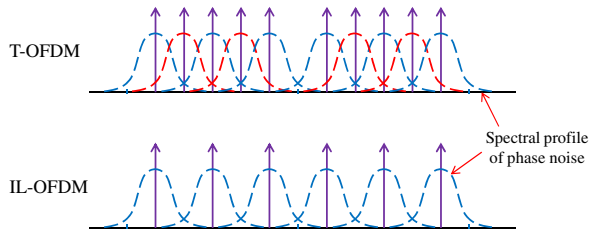

Fig. 1. Phase noise induced intercarrier interference of traditional OFDM and interleaved OFDM.

$$S(n) = \frac{1}{N}\sum_{k=0}^{0.5*N-1} X_{2k+1} e^{j2\pi\frac{(2k+1)n}{N}}, \qquad n = 0, 1, 2, \ldots, N-1. \tag{2}$$

The symmetry property of the IL-OFDM can be verified as

$$\begin{aligned} S\left(n+\frac{N}{2}\right) &= \frac{1}{N}\sum_{k=0}^{0.5*N-1} X_{2k} e^{j2\pi\frac{2k*(n+N/2)}{N}}, \\ &= \frac{1}{N}\sum_{k=0}^{0.5*N-1} X_{2k} e^{j2\pi\frac{2kn}{N}+2\pi k}, \\ &= S(n). \end{aligned} \tag{3}$$

The corresponding analog expression is

$$S\left(t+\frac{T_{\mathrm{IL}}}{2}\right) = S(t), \qquad t \in \left(0, \frac{T_{\mathrm{IL}}}{2}\right], \tag{4}$$

where T_{IL} denotes the period of one IL-OFDM symbol. It suggests that the waveform of the IL-OFDM is periodic. To form a PT-IL-OFDM waveform, the waveform of the IL-OFDM is truncated by only transmitting its first half. When the PT-IL-OFDM signal is received the operation of waveform reconstruction is performed to duplicate the received waveform. After the waveform reconstruction, the PT-IL-OFDM waveform is back to its corresponding IL-OFDM waveform. Now it is clear that the realization of a PT-IL-OFDM signal is the same as one from the IL-OFDM except for the waveform truncation and the reconstruction.

Here, the numerical simulation is carried out to investigate the properties of the IL-OFDM and PT-IL-OFDM. The simulation platform is shown in Fig. 2. The optical carrier generated from a laser source passes to an IQ modulator (IQ-MOD in Fig. 2). The I and Q components of an OFDM signal are then modulated on the I and Q components of the optical carrier, as shown in Fig. 2. There are two steps to generate an OFDM signal, digital signal processing (DSP) and digital to analog conversion (DAC). The detailed DSP for the transmitter (DSP-Tx) is shown in Fig. 2. The pseudo random binary sequence is generated. Then, the binary sequence is Gray encoded and mapped to the complex symbols for all used subcarriers. The subcarriers are allocated as normally (T-OFDM) or interleaved [(PT)-IL-OFDM)]. The pilots are inserted for the estimation of the channel response and of the CPE induced by the phase noise. After the IDFT for OFDM modulation (here we use IFFT, or inverse fast Fourier transform) and, adding a cyclic prefix, a data OFDM symbol is realized. The additional operation of waveform truncation is applied for PT-IL-OFDM. After many iterations of the above operations a frame of data OFDM symbols is generated. A training sequence is added in front for timing and frequency offset estimation. Finally, the parallel to serial conversion of the digital samples is performed and is further converted to the analog signal. On the receiver side the arrived optical signal is amplified via an ideal optical amplifier (OA in Fig. 2), and then is mixed with the optical carrier from the OLO via a 90° optical hybrid. The I and Q components of the mixed optical signals are then converted to the electrical signals via the balanced photodiodes (B-PDs shown in Fig. 2). After the analog-to-digital conversion (ADC), the DSP (DSP-Rx) is performed to retrieve the transmitted data with the details shown in Fig. 2. The time and frequency offset estimation is applied to the retrieved signal using the training sequence. After the frequency offset compensation (FOC shown in Fig. 2), the additional operation of waveform reconstruction is employed for the PT-IL-OFDM. The cyclic prefix is removed and a fast Fourier transform (FFT) operation is performed to demodulate the OFDM symbols. The channel response and CPE estimated from the pilots are equalized before the error vector magnitude (EVM) calculations. The detailed parameters for T-OFDM, IL-OFDM, and PT-IL-OFDM are presented in Table 1. Here, the (I)FFT size is chosen to be 64 as a trade-off between the implementation complexity and spectral flexibility. The detailed

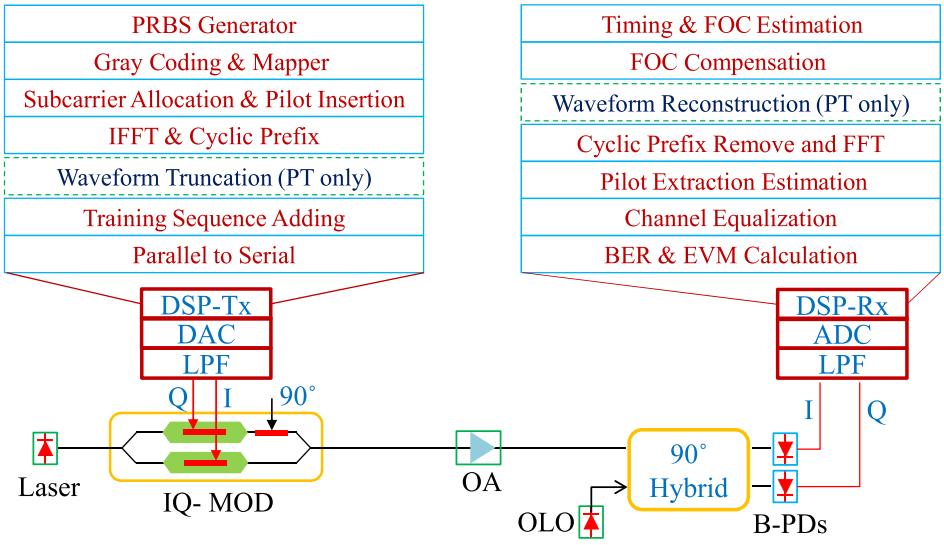

Fig. 2. Simulation principle of traditional OFDM (T-OFDM), interleaved OFDM (IL-OFDM), and partial transmission IL-OFDM (PT-IL-OFDM).

Table 1. Parameters of OFDM Modulations[a]

Items	Sub Items	Values
OFDM symbol	FFT size	64
	Subcarrier number	50
	Subcarrier modulation	QAM-16
	Modulated subcarrier	50 for T 25 for IL & PT
	Pilots number	4
	Cyclic prefix	8 for T & IL 4 for PT
	Initial subcarrier	1
	Symbol length	72 for T & IL 36 for PT
OFDM frame	OFDM symbol	200 for Fig. 3 50 for Fig. 4
	Frame number	50 for Fig. 3 1 for Fig. 4

[a]T, traditional OFDM; IL, interleaved OFDM; PT, partial transmission interleaved OFDM.

physical parameters are presented in Table 2. The simulations for PAPR analysis and phase noise induced ICI are presented as follows.

The PAPRs of T-OFDM, IL-OFDM, and PT-IL-OFDM are calculated from the generated waveforms in terms of the complementary cumulative distribution function (CCDF). The simulation includes 50 OFDM frames. Each OFDM frame incorporates 200 OFDM symbols. Thus, the total amount of simulation symbols is 1×10^4. The PAPRs are directly calculated in the digital domain. The complex samples of an OFDM signal are multiplied with their corresponding conjugate values to calculate the individual power values for all the samples. The max power value is searched for and then divided into the average of all the power values. Then, a histogram process is performed before the cumulative distribution analysis. Since 1×10^4 symbols are employed, the max probability of 1×10^{-4}

Table 2. Physical Parameters

IQ-MOD	Vpi	4 V
	Extinction ratio	25 dB
	Insertion loss	5 dB
	Phase between I and Q	90
PD	Electrical bandwidth	20 GHz
	Responsivity	100 A/W
Optical hybrid	Insertion loss	1 dB
	Phase between I and Q	90
Optical power	In fiber	3 dBm
	Out fiber	−23 dBm
	In PD	1 dBm
Laser (Tx)	Wavelength	193.1 THz
	Power	16 dBm
	Linewidth	100–400 kHz
OLO	Wavelength	193.1 THz
	Power	25 dBm
	Linewidth	100–400 kHz
DAC	Sample Rate	12.3 GSa/s
	Low pass filter	6 GHz
	Amplitude (Vpp)	4 V
ADC	Sample rate	12.3 GSa/s
	Low pass filter	6 GHz
OFDM	Bit rate	28.5 Gbps
	Bandwidth	4.8 GHz

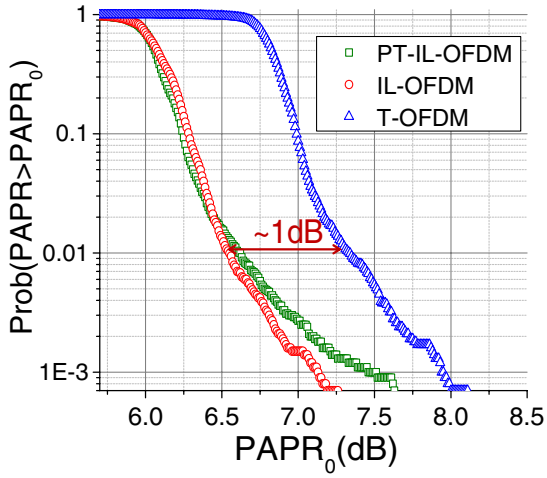

Fig. 3. CCDF for T-OFDM, IL-OFDM, and PT-IL-OFDM.

can be obtained. As mentioned before, the related OFDM parameters are shown in Table 1. Figure 3 shows the CCDF of PAPRs for T-OFDM, IL-OFDM, and PT-IL-OFDM. We can, obviously, find that the PAPRs of IL-OFDM and PT-IL-OFDM are 0.75 dB lower than the one of T-OFDM for 99% of the symbols (0.01 in the y axis). Note that no distortion is introduced for such PAPR reduction.

Here, the PN-ICI tolerances of T-OFDM, IL-OFDM, and PT-IL-OFDM are evaluated based on their EVMs versus different linewidths. The powers of the transmitter laser and the OLO are 16 and 25 dBm, respectively. The relative intensity noises (RINs) of both the transmitter laser and the OLO are −155 dB/Hz at 10 dBm laser output power. All three types of OFDM signals are modulated on the E-field of the optical carrier through the IQ-MOD. The subcarrier power of all the OFDM signals is equalized. The switch voltage (Vpi), insertion loss, and extinction ratio for the IQ modulator are 4 V, 5 dB, and 25 dB, respectively. The optical signal after the IQ modulator is equalized to 3 dBm for three OFDM signals via an ideal optical amplifier. The B-PDs are used to eliminate the DC component and the second-order distortion. Its sensitivity is intentionally set to 100 A/W to include the electrical amplification. Its thermal noise and dark current are −174 dBm/Hz and 10 nA, respectively. The shot noise of the B-PDs is a Gaussian distribution. The FWHM linewidths of the transmitter side (Laser in Fig. 2) and the OLO side are identical. Since the final phase noise incorporates the contributions from both sides, the following discussion is based on combined linewidths. The linewidth of both sides varies from 100 to 400 kHz with a step of 100 kHz. Thus, the combined linewidth varies from 200 to 800 kHz with a step of 200 kHz. The detailed parameters are shown in Tables 1 and 2. As shown in Fig. 4, the EVMs for three types of OFDM signals are evaluated versus the combined linewidths. In general, IL-OFDM and PT-IL-OFDM exhibit better tolerance toward phase noise than T-OFDM. The EVMs of IL-OFDM and PT-IL-OFDM are 5.4 and 3.1 dB better than that of T-OFDM with the same combined linewidths. The tolerance of PT-IL-OFDM is observed to be worse than IL-OFDM, as shown in Fig. 4, due to the imperfect waveform reconstruction. The gaps

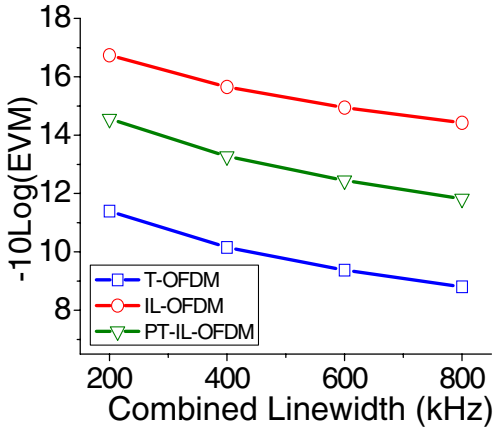

Fig. 4. EVMs of T-OFDM, IL-OFDM, and PT-IL-OFDM versus combined linewidths.

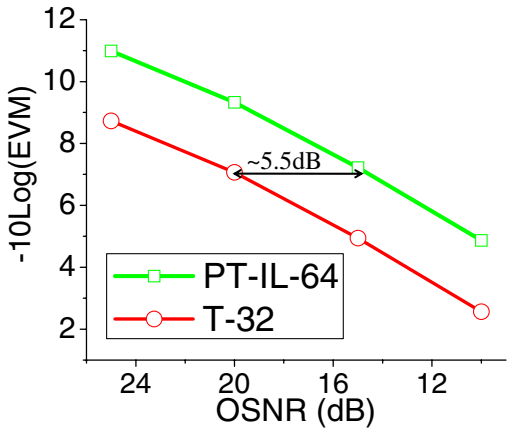

Fig. 5. EVMs of PT-IL-OFDM ((I)FFT size = 64), T-OFDM ((I) FFT size = 32) versus OSNRs.

among the three curves are constant over a wide range of combined linewidths, which means that the PN-ICI tolerance improvement of IL-OFDM and PT-IL-OFDM toward T-OFDM is constant. It exhibits its suitability for various applications.

As shown in Fig. 5, the performance of a PT-IL-OFDM signal with a (I)FFT size of 64 (PT-IL-64) is compared with a T-OFDM signal with a (I)FFT size of 32 (T-32). The combined linewidths of both are identically set to 400 kHz. Other parameters can be found in Table 2. Both EVMs of PT-IL-OFDM and T-OFDM signals are increased when their optical signal to noise ratios (OSNRs) are decreased. The PT-IL-OFDM signal exhibits a constantly better performance than the T-OFDM. To obtain −7 dB EVM for both signals, the PT-IL-OFDM requires an OSNR 5.5 dB lower than T-OFDM. This suggests that the PT-IL-OFDM does gain advantages toward T-OFDM with the (I) FFT size halved.

Here, we conclude the whole Letter. A novel group of interleaved orthogonal frequency division multiplexing (IL-OFDM) and partial transmission IL-OFDM (PT-IL-OFDM) schemes are proposed for optical coherent detection. The numerical simulations show that the IL-OFDM and PT-IL-OFDM can gain a 0.75 dB reduction of the PAPR against traditional OFDM (T-OFDM). Compared with T-OFDM, the PN-ICI tolerances are 5.2 and 3.1 dB improved for IL-OFDM and PT-IL-OFDM, respectively.

This work is supported by The Netherlands Organization for Scientific Research (NWO) under the project grant Smart Optical-Wireless In-home Communication Infrastructure (SOWICI).

References

1. X. Liu, F. Buchali, and R. W. Tkach, J. Lightwave Technol. **27**, 3632 (2009).
2. A. J. Lowery, L. B. Du, and J. Armstrong, J. Lightwave Technol. **25**, 131, 2007.
3. W. Peng, B. Zhang, K. Feng, X. Wu, A. E. Willner, and S. Chi, J. Lightwave Technol. **27**, 5723 (2009).
4. A. J. Lowery, Opt. Express **15**, 12965 (2007).
5. J. Armstrong, J. Lightwave Technol. **27**, 189 (2009).
6. X. Yi, W. Shieh, and Y. Ma, J. Lightwave Technol. **26**, 2578 (2008).
7. S. Randel, S. Adhikari, and S. L. Jansen, IEEE Photon. Technol. Lett. **22**, 1288 (2010).
8. J. Zhao and A. D. Ellis, *Optical Fiber Communication Conference*, OSA Technical Digest (Optical Society of America, 2010), paper OMR1.9.
9. Q. Yang, Y. Tang, Y. Ma, and W. Shieh, J. Lightwave Technol. **27**, 168 (2009).
10. S. L. Jansen, I. Morita, T. C. W. Schenk, and H. Tanaka, J. Lightwave Technol. **27**, 177 (2009).
11. A. Li, X. Chen, G. Gao, and W. Shieh, J. Lightwave Technol. **30**, 3931 (2012).
12. D. Qian, N. Cvijetic, J. Hu, and T. Wang, IEEE Photon. Technol. Lett. **21**, 1265 (2009).
13. J. Yu, M. Huang, D. Qian, L. Chen, and G. K. Chang, IEEE Photon. Technol. Lett. **20**, 1545 (2008).
14. Z. Cao, J. Yu, W. Wang, L. Chen, and Z. Dong, IEEE Photon. Technol. Lett. **22**, 691 (2010).
15. S. C. J. Lee, S. Randel, F. Breyer, and A. M. J. Koonen, IEEE Photon. Technol. Lett. **21**, 1749 (2009).
16. S. C. J. Lee, F. Breyer, S. Randel, D. Cardenas, H. P. A. van den Boom, and A. M. J. Koonen, in *Optical Fiber Communication Conference*, OSA Technical Digest (Optical Society of America, 2009), paper OWM2.